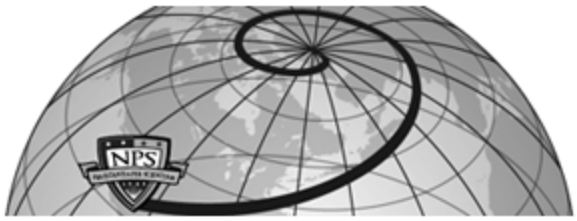

DESIGN OF AN AUTOMATIC FLUX LEVEL CONTROL SYSTEM FOR THE AGN-201 REACTOR

* * * * *

George M. Gans, Jr.

DESIGN OF AN AUTOMATIC FLUX LEVEL CONTROL SYSTEM FOR THE AGN-201 REACTOR

by

George M. Gans, Jr.

Lieutenant, Civil Engineer Corps, United States Navy

Submitted in partial fulfillment of
the requirements for the degree of

MASTER OF SCIENCE
IN
NUCLEAR ENGINEERING

United States Naval Postgraduate School
Monterey, California

1 9 6 3

DESIGN OF AN AUTOMATIC FLUX LEVEL CONTROL SYSTEM FOR THE AGN-201 REACTOR

by

George M. Gans, Jr.

This work is accepted as fulfilling
the thesis requirements for the degree of

MASTER OF SCIENCE

IN

NUCLEAR ENGINEERING

from the

United States Naval Postgraduate School

Alex Gerba Jr.
Faculty Advisor

R. E. Newton
Chairman
Department of Mechanical Engineering

Approved:

W. F. Koehler
Academic Dean (Acting)

TABLE OF CONTENTS

LIST OF ILLUSTRATIONS

TABLE OF SYMBOLS AND ABBREVIATIONS

Symbol	Definition	Units
B^2	Geometric buckling	cm^{-2}
C_i	Density of the ith group of delayed neutron precursors	$specie/_{cm^3}$
D	Diffusion Coefficient for core material	cm
k_∞	multiplication factor for infinite medium	none
k_{eff}	Effective multiplication factor for finite medium	none
δk	Reactivity	reactivity units
δk_1	Reactivity	dollars
δk_D	Reactivity from a disturbance	reactivity units
δk_R	Reactivity produced from rod movement due to controller action	reactivity units
L	Thermal diffusion length of core material	cm
l_o	mean lifetime of thermal neutrons in an infinite reactor	sec
l	mean lifetime of thermal neutrons in a finite reactor	sec
n, n(t)	Neutron density	n/cm^3
n_1	Normalized neutron density, n(t)/n(o)	none
$\triangle n$	The variation of the density from its initial value, n(t) - n(o)	n/cm^3
n_o	Same as n(o), the initial steady value of neutron density. Also the set reference, the desired power level.	n/cm^3
p	Resonance escape probability	none
T	Reactor period	sec

Symbol	Definition	Units
t	Real time	sec.
v	Mean velocity of thermal neutrons	cm/sec.
β	Delayed neutron fraction	none
∇^2	Laplacian operator	cm^{-2}
γ	Average delayed neutron effectiveness for the six groups	none
γ_i	Effectiveness for the ith group	none
Γ	A dimensionless parameter which appears in the derivation of expression for k_{eff} (See Appendix A)	none
ϵ	Fast fission factor	none
ν	Average number of neutrons emitted per fission (2.46 for U^{235})	neutrons/fission
λ_i	Decay constant for the ith group of delayed neutron emitters	sec^{-1}
ϕ	Neutron flux	n/cm^2-sec.
Σ_a	Energy-averaged macroscopic neutron absorption cross section	cm^{-1}
Σ_f	Fission cross section	cm^{-1}
Σ	"Sigma", the summation Symbol	none
τ_d	Fermi age for delayed neutrons	cm^2
τ_p	Fermi age for prompt neutrons	cm^2
$[\ ]'$	Prime denotes analog computer voltage representation of quantity indicated	none

1. Introduction.

The AGN-201 reactor is a low power reactor which was produced in quantity by Aerojet-General Nucleonics for use in education, research, medical diagnosis, and industrial process control [7]. The 25 by 25 cm. cylindrical core is constructed of discs of a homogeneous mixture of polyethylene moderator and UO_2, which is 20% enriched in U^{235}. The critical mass is 656 grams of U^{235} dispursed in approximately 11 Kg. of polyethylene. Control of the reactor is accomplished by four fuel-loaded control rods, two act as safety rods, and two operate as control rods. The original licensed power was 0.1 watt but shielding modifications now permit the reactor at the U. S. Naval Postgraduate School to operate at 1000 watts. At this power, a maximum flux of about 5×10^{10} n/cm^2-sec. is available in a "glory hole" which penetrates the core to its center.

The reactor is used by the Postgraduate School for a variety of purposes. One of the largest uses is for the neutron activation of various chemical elements. This operation involves the maintenance of a steady power level for extended periods of time. An automatic system capable of maintaining the neutron flux (reactor power) at a preset level would reduce operator fatigue and free him from the simple task of manipulating a switch to keep a meter reading constant. This automatic operation would permit him to observe more closely the overall behavior of the reactor. The objective of this thesis work was to design such a control system. The approach to the design was to investigate the time behavior of the AGN-201, simulate that time behavior on an analog computer and use the analog simulation as an experimental tool in the design of the control system.

The specifications for the automatic flux control system, hereafter abbreviated as the AFC system, were established as follows:

1. The system will be capable of maintaining stable operation at any desired flux (power) level between 0.01 watts and 200 watts.
2. Accuracy of control will be within $\pm$ 1% of a set power level.
3. The neutron detection systems and control and safety circuits of the reactor will not be disturbed or changed by the AFC system.
4. Control of the reactor will be effected by using the existing control rod actuators and the rates of travel of the rods will not be changed. This specification stems from an agreement with the Atomic Energy Commission regarding the proposed AFC system.
5. Override of the AFC system will be possible by manipulating the manual controls of the reactor.
6. The AFC system will be made as safe as possible against failure of its components. That is, failure of a vacuum tube or relay will not cause insertion of positive reactivity into the reactor.

2. Type of System and Design Methods Used.

The control problem may be explained by reference to Fig. 1. See Section 5 for a detailed description of the AFC system.

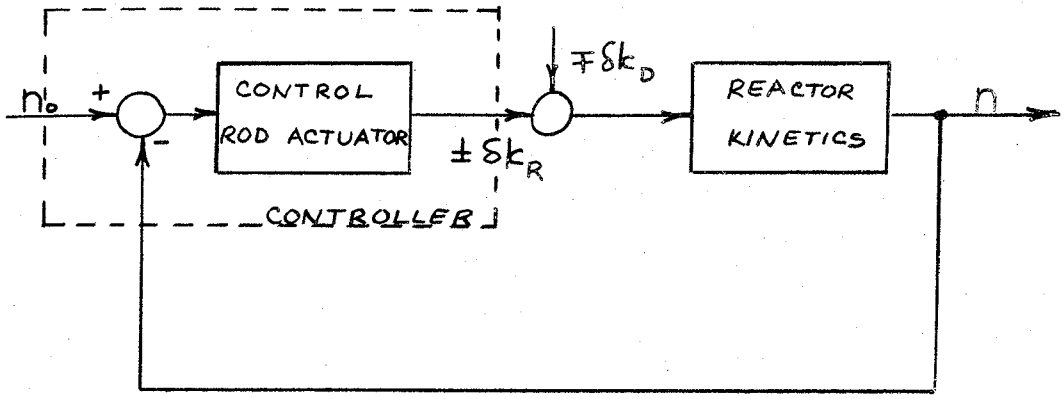

Fig. 1 Block Diagram of the Control Problem.

It is the function of the AFC system to compare the reactor neutron density[1], n, with a reference level, n_o. If an error is found to exist, the system will initiate control rod action so that rod reactivity, δk_R, is changed in the proper direction to bring the error to zero. The possibility exists for a reactivity disturbance, δk_D, to be introduced during the performance of an experiment on the reactor. Regardless of the interaction of δk_R and δk_L, the actuator must be designed to reduce the error as long as an error exists.

The system specifications described above indicate the desirability of using a discontinuous, on-off, type control system. Specification 4

[1] Neutron density, flux and power will be used interchangeably in this report.

is particularly restricting. In order to use a continuous controller we must have the capability of varying the corrective action. As applied to the AGN-201, this means variable rod speed. Without this capability, our choice is limited to a form of discontinuous controller which can perform in a satisfactory manner using fixed control rod speed. Actually, each control rod on the AGN has two speeds but this is not enough flexibility for a continuous control system. A continuous controller provides continuous corrective action [4] . This would be unwise for a control rod drive mechanism, like that on the AGN-201, that was not specifically designed for continuous duty. The AGN rod drive motors are 1/25 HP, 115VDC, Shunt motors, rated for intermittent service only. In adhering to the specification to avoid changes in the rod actuator, a further consideration is the fact that a power amplifier would be required with a continuous control system. The addition of an amplidyne or other amplification device would require major and expensive changes in the motor wiring of the reactor. A discontinuous controller does not require a power amplifier. Amplification is effectively provided through the action of relays.

Aside from these specific considerations, the desirability of using a discontinuous contactor type system for the control of nuclear reactors has been illustrated in the past [16] [17] [23] . For the reasons described above, it was decided to design a discontinuous, on-off, type control system.

The analytical approach to the design of a control system has been described in detail in textbooks on control [9] [24] . Working with the differential equations or transfer function which describes the behavior of the plant, the engineer can analytically design a controller to

make a system perform as required. Design methods favoring experimental techniques are also used in control work. After a plant transfer function has been determined or a series of differential equations devised that apply to the plant, a simulation device can be fashioned that will behave in a manner similar to the plant which is to be controlled. The actual equipment of the proposed control system can be operated with the simulation device and direct evaluation of the ability of the system to meet the design specification can be made. System parameter changes can be readily tested with the simulation thereby simplifying the optimization of the control system design.

In the investigation at hand, there were several factors which tended to favor the experimental approach to the design problem. The time behavior of a nuclear reactor is nonlinear. That is, one of the seven differential equations which describe the kinetic behavior of a reactor contains a nonlinear term. In Section 3, Reactor kinetic equations, equation (2) shows the product of the multiplication factor, k_{eff} and neutron density, n. Neutron density is dependent upon k_{eff}. A transfer function, by definition, describes linear behavior. If a system is to be treated by analytical methods using transfer functions, it must be made linear. Using small signal techniques, the reactor equations can be made linear and a transfer function obtained [2]. The result is a seventh order polynomial which describes the behavior of the reactor reasonably well under conditions of small disturbances [23]. For large disturbances, the linear approximation introduces gross errors in the time response. No approximations of this type are necessary in a plant simulation. Specifically, an electronic representation of the

differential equations of a nuclear reactor can easily handle the non-linear term described above by the use of a function multiplier.

The choice of a discontinuous type controller also influences the design approach to be used. Describing function techniques can be used to approximate relay behavior in order that linear design methods may be applied to the problem [17] [23]. However, the method based on describing functions provides little information about transient behavior [10]. Phase plane analysis has been applied to the design of nonlinear systems but its application is limited, for computational reasons, to second order systems [25]. Using a simulated control system or the actual control system itself in a closed loop with the plant simulation, eliminates the necessity of the above approximations and offers the designer a direct, accurate measurement of the behavior of the actual control system.

Fig. 1 shows two inputs to the system, n_o and δk_D. In the analysis of such a system the effect of more than one input on the system behavior is determined by considering the effect of each input separately and then applying the principle of superposition. [9]. This approach presumes prior application of linearization approximations to a non-linear problem. With an experimental design approach, using a plant simulation, no serious problems are posed by a variety of inputs.

To avoid the approximations described above and to keep the complexity of the design problem at a minimum, it was decided to apply the simulation approach to the design. Specifically, the differential equations describing the kinetic behavior of the AGN-201 were programmed on the electronic analog computer and the computer simulation was used as a design

tool in choosing and optimizing the components for a control system.

In order to have reasonable assurance that the simulation accurately represented the actual behavior of the AGN-201, two methods of checking the simulation were used; comparison with a digital solution of the reactor kinetic equations, and comparison with the actual behavior of the reactor itself. One might presume that comparison with the reactor would be sufficient proof of the validity of the simulation. Unfortunately exact comparison was not possible for several reasons. One reason was related to the problem of applying a true step input of reactivity. However, a reasonable "forced fit", described in Section 4, was made and the accuracy of the analog simulation was established.

Utilization of a device that simulated the reactor behavior offered several advantages to the designer over the use of the reactor itself. Foremost was the lack of problems of nuclear safety. The nuclear chain reaction requires constant supervision and control. Many control devices, if used improperly, go into a saturated condition or damage a readily replacable component. A nuclear reactor however, if allowed to get out of control, presents radiological safety hazards to personnel and can do costly damage to itself. A second advantage of a simulated reactor is ease of operation. An analog computer can be stopped, reset and restarted without delay. A nuclear reactor, on the other hand, requires elaborate checkout procedures prior to starting and requires a considerable amount of time to shut down or return to a stable power level for a new run. After the initial set-up is accomplished, an analog computer can be operated repeatedly without any delay other than for the setting of a potentiometer or changing some other controller parameter for a new run.

3. Reactor Kinetic Equations.

The nuclear reactor kinetic equations used in this report are derived in this section. The developed equations are shown here;

$$\frac{dn}{dt} = \frac{n}{\ell}\left[\frac{(1-\beta)\,k_{eff} + \beta(1-\gamma) - 1}{\Gamma}\right] + p e^{-B^2\tau_p} \sum_{1}^{6} \gamma_i \lambda_i C_i \tag{2}$$

$$\frac{dC_i}{dt} = \frac{\beta_i k_{eff}\, n}{\Gamma \ell}\left(\frac{1}{p e^{-B^2\tau_p}}\right) - \lambda_i C_i \tag{4}$$

$$i = 1, 2, 3 \ldots 6$$

For definitions of the terms used, the reader is referred to the Table of Symbols and Abbreviations, page v.

The above equations are simply the expressions describing the time behavior of the thermal neutrons in the reactor. These expressions can be derived by considering the sources (production) and sinks (losses) of thermal neutrons. Thus, in equation form, per unit volume,

Rate of change of neutron density = Rate of production - Rate of losses.

The two sources of thermal neutrons are the prompt and delayed neutrons that have been slowed down. Also there are two general processes causing loss of neutrons in a reactor, absorption and leakage[1]. We may

[1]Absorption refers to the nuclear reaction whereby a neutron is captured by the nucleus of some material present. Some of the captures result in fission, others produce gamma rays or other non-productive results. Leakage refers to the escape of neutrons from the reactor system without reacting with (being captured by) a nucleus.

now write

$$dn/dt = S_p + S_d - LR - AR$$

where

S_p = production rate from prompt neutrons

S_d = production rate from delayed neutrons

LR = leakage rate of neutrons

AR = absorption rate of neutrons

The four terms will be described. Rather than starting from first principles, it will be assumed that the reader is familiar with the fundamentals of reactor theory as contained in the textbook by Glasstone & Edlund [14]. This reference should be consulted for more detailed information. From reactor theory, the neutron behavior is both time and space dependent. The space-independent form of the expressions will be used. Therefore we will concern ourselves only with the time varying aspects of the quantities. The production rate from prompt neutrons is given by the expression,

$$S_p = (1-\beta)\, k_\infty \Sigma_a e^{-B^2\tau_p} \phi$$

The production rate from delayed neutrons is,

$$S_d = \sum_{i=1}^{6} p_i\, e^{-B^2\tau_{di}} \lambda_i C_i$$

$$= p e^{-B^2\tau_p} \sum_{i=1}^{6} \gamma_i \lambda_i C_i$$

where γ_i is the delayed neutron effectiveness and is defined by the expression

$$\gamma_i = \frac{e^{-B^2\tau_{di}}}{e^{-B^2\tau_p}}$$ See Appendix A

We note that $p_i = p$ since the delayed neutrons are emitted at energies above the major resonances of U^{238}.

The leakage and absorption rates for the neutrons are,

$$LR = -D\nabla^2\phi$$

$$AR = \Sigma_a \phi$$

The combined equation becomes

$$\frac{dn}{dt} = (1-\beta)k_\infty \Sigma_a e^{-B^2\tau_P}\phi + p e^{-B^2\tau_P}\sum_1^6 \gamma_i \lambda_i C_i \qquad (1)$$

$$-(-D\nabla^2\phi) - \Sigma_a \phi$$

This equation can be arranged in a more useful form by applying the following definitions [14] .

$$\phi = nv \qquad l_o = \frac{1}{\Sigma_a v} \qquad l = \frac{l_o}{1+L^2B^2}$$

$$L^2 = \frac{D}{\Sigma_a} \qquad \nabla^2\phi = -B^2\phi$$ (this follows from space - independence assumption)

$$k_{eff} = \frac{k_\infty e^{-B^2\tau_P}\Gamma}{1+L^2B^2}$$ See Appendix A

Substitution of these expressions into eq. (1) and simplifying,

$$\frac{dn}{dt} = \frac{n}{l}\left[\frac{(1-\beta)k_{eff} + \beta(1-\gamma) - 1}{\Gamma}\right] \qquad (2)$$

$$+ p e^{-B^2\tau_P}\sum_1^6 \gamma_i \lambda_i C_i$$

Equation (2) contains seven unknowns, the six delayed neutron precursors (the C_i's) and the neutron density (n). Six more equations are obtained from the rates of change of the precursors. In equation form,

dC_i/dt = Production Rate - Decay Rate

$i = 1, 2, \ldots 6$

or,

$$\frac{dC_i}{dt} = \beta_i \in \nu\Sigma_f \phi - \lambda_i C_i \qquad (3)$$

Making substitutions similar to those made in eq. (1),

$$\frac{dC_i}{dt} = \frac{\beta_i k_{eff}}{\Gamma} \frac{n}{l} \left(\frac{1}{\rho e^{-B^2 \tau_p}} \right) - \lambda_i C_i \qquad (4)$$

$$i = 1, 2, \ldots . 6$$

Γ has a value of 1.0009 for U^{235} with $\gamma = 1.14$ and will be approximated by unity in all further expressions.

The seven equations made up of (2) and (4) are the kinetic equations of the nuclear reactor. These equations will be used in Section 4 in setting up the analog computer solution and in programming the digital solution.

4. Simulation of the Nuclear Reactor.

The actual design and testing of components of the flux controller was accomplished using an analog computer simulation of the kinetic equations of the AGN-201. Appendix B contains details of the analog computer set-up.

The computer used was a Donner Model 3100, containing 30 amplifiers [11]. A Donner Model 3735 electronic multiplier was used to obtain the product of the two time-varying quantities mentioned in Section 2. The 3100 has 15 amplifiers suitable for use as integrators or as summer-inverters and 15 amplifiers which can be used as summer-inverters only. 40 ten-turn helipot potentiometers, four of which are ungrounded, are included in the computer.

The solution used in this investigation required 11 integrators, 15 summer-inverters and 39 potentiometers. See Schematic Drawing in Appendix B.

Two programming problems, relating to magnitude scaling, made the resulting computer set-up rather intricate and unwieldly. First of all, the use of an inherently drift-prone electronic multiplier required special effort to arrange scaling of the problem so that the input voltages to the multiplier were as near as practicable to the maximum allowable of 100V. This technique, including the division of the multiplier output by a large factor before using it in the rest of the solution, eliminated the problem of multiplier drift from practical consideration. Secondly, the wide differences between the coefficients of the differential equations required some very small potentiometer settings. In order to achieve maximum accuracy of simulation, additional fractional inverters (amplifiers 18 and 19, for example) were used to avoid potentiometer

settings near the extreme limits of arm travel.

The scaling requirements mentioned above resulted in a limitation of the time duration for a computer run. When the analog was operated by itself without any controlling action being applied to it, overloading of several amplifiers occurred after 20 to 30 seconds, depending upon the magnitude of the step disturbance used. This was not a serious limitation since the solution was not permitted to stray far from equilibrium when the analog was placed in closed-loop operation with the controller.

The computer equations used were derived from the kinetic equations previously developed. Reference 3 was used as a guide in this work. From Section 3, the kinetic equations are:

$$\frac{dn}{dt} = \frac{n}{\ell}\left[k_{eff}(1-\beta) + \beta(1-\gamma') - 1\right] + p e^{-B^2 T_p} \sum_{i}^{6} \lambda_i \gamma_i C_i \tag{2}$$

$$\frac{dC_i}{dt} = \beta_i k_{eff} \frac{n}{\ell}\left(\frac{1}{p e^{-B^2 T_p}}\right) - \lambda_i C_i \qquad i = 1,2,\ldots 6 \qquad \Gamma \cong 1 \tag{4}$$

At the steady-state equilibrium condition,

$$\frac{dC_i}{dt} = 0 \quad , \; k_{eff} = 1 \; , \quad C_i = C_i(0) \; , \quad n = n(0)$$

Equation (4) then becomes,

$$0 = \frac{\beta_i n(0)}{\ell}\left(\frac{1}{p e^{-B^2 T_p}}\right) - \lambda_i C_i(0)$$

Thus,

$$C_i(0) = \left[\frac{\beta_i}{\lambda_i \ell p e^{-B^2 T_p}}\right] n(0) \tag{5}$$

The coefficients in eq. (2) and (4) differ widely in magnitude, thus it is convenient to redefine the variables as follows,

$$n_1 = \frac{n(t)}{n(0)}$$

$$C_{i1} = \frac{C_i(t)}{C_i(0)} \qquad (6)$$

$$\delta k_1 = \frac{\delta k}{\beta} = \frac{(k_{eff}-1)}{\beta}^{1} \quad \text{(dollar units)}$$

Substituting (5) and (6) into (2) and (4) yields

$$\frac{dn_1}{dt} = \frac{\beta n_1}{\ell}\left[\delta k_1(1-\beta) - \gamma\beta\right] + \frac{1}{\ell}\sum_1^6 \gamma_i \lambda_i C_{i1} \qquad (2')$$

$$\frac{dC_{i1}}{dt} = \beta(\delta k_1 + 1)\lambda_i n_1 - \lambda_i C_{i1} \qquad (4')$$

The normalized n and C can be written in the following forms,

$$n_1 = 1 + \Delta n_1$$

$$C_{i1} = 1 + \Delta C_{i1} \qquad \text{(Footnote 2)} \qquad (7)$$

By using this form, it is possible to operate only on the non-equilibrium portion of the variables. This further reduces the effect of any multiplier drift. Note that

$$\frac{dn_1}{dt} = \frac{d\Delta n_1}{dt}$$

and

$$\frac{dC_{i1}}{dt} = \frac{d\Delta C_{i1}}{dt}$$

The substitution of (7) into (2') and (4') yields

$$\frac{\ell}{\beta}\frac{d\Delta n_1}{dt} = \delta k_1(1-\beta) + \Delta n_1 \delta k_1(1-\beta) - \gamma\Delta n_1 + \frac{1}{\beta}\sum_1^6 \gamma_i \beta_i \Delta C_{i1} \qquad (2'')$$

$$\frac{d\Delta C_{i1}}{dt} = \lambda_i \beta \delta k_1 + \lambda_i \beta \Delta n_1 \delta k_1 + \lambda_i \Delta n_1 - \lambda_i \Delta C_{i1} \qquad (4'')$$

[1] We are using here the approximation that reactivity, δk, is equal to $(k_{eff}-1)$. The precise definition is $(k_{eff}-1)/k_{eff}$. The maximum error caused by this approximation is less than 1% when $k_{eff} = 1.0064$, at prompt critical.

[2] Δn_1 and ΔC_{i1} are variational changes of the normalized quantities from unity.

Machine voltage representation of the variables is computed by using conventional scaling factors. The prime denotes machine voltages.

$$t' = at$$
$$n_1' = b\, n_1$$
$$C_{i_1}' = g_i C_{i1}$$
$$\delta k_1' = e\, \delta k_1$$

The final form of the kinetic equations suitable for direct simulation on an electronic analog computer is

$$\left[\frac{10\ell a}{\beta}\right]\frac{1}{10}\frac{d\Delta n_1'}{dt'} = \left[\frac{b(1-\beta)}{e}\right]\delta k_1' + \left[\frac{1-\beta}{e}\right]\Delta n_1'\,\delta k_1' - [\gamma]\Delta n_1' + \left[\frac{b}{\beta g}\right]\sum_1^6 \gamma_i \beta_i \Delta C_{i_1}' \tag{8}$$

$$\frac{d\Delta C_{i_1}'}{dt'} = \left[\frac{\lambda_i \beta g}{ae}\right]\delta k_1' + \left[\frac{\lambda_i \beta g}{eab}\right]\Delta n_1'\,\delta k_1' + \left[\frac{\lambda_i g}{ab}\right]\Delta n_1' - \left[\frac{\lambda_i}{a}\right]\Delta C_{i_1}' \tag{9}$$

The following scaling factors were found convenient for this application,

a = 1 volt/sec.

b = 10 volts/normalized neutron density.

g_i = g = 100 volts/normalized precursor density

e = 20 volts/dollar reactivity.

Because the $\Delta n_1'$ and $\Delta C_{i_1}'$ form of the variables was used, the initial conditions were zero for all the integrators.

The conventional transfer function for a motor driven device is $\frac{1}{s(sT_m+1)}$. Where T_m represents the time constant of the device. Since equipment was not available for measuring T_m and since the rods on the

AGN are small and are driven through a high gear ratio, an estimated value of 0.1 was assigned to τ_m. It was known that the control rod was operating on the linear portion of the rod calibration (reactivity vs rod position) curve. See Appendix B for details of the rod simulation. Using the measured speed of travel and knowing the linear worth of the rods, the reactivity rate of the two control rods was determined.

	δk_R/sec.
Fine Control Rod	
Slow Speed	0.282×10^{-4}
Fast Speed	0.860×10^{-4}
Coarse Control Rod	
Slow Speed	1.71×10^{-4}
Fast Speed	2.90×10^{-4}

The computer scaled quantity becomes

$$\delta k'_{1R} = \frac{e}{\beta} \delta k_R = 0.311 \times 10^{-4} \delta k_R = e_R$$

Two checks were made on the accuracy of simulation. Since the design of the control system was based on the performance of the system with the analog simulation, every effort was made to achieve a simulation that accurately duplicated the reactor behavior. One check consisted of comparison of the analog solution with a digital computer solution of the time response of a nuclear reactor. The other check consisted of fitting the analog solution to the actual measured behavior of the reactor itself. A description of the latter check procedure is given later in this section.

With regard to the digital computer check method, Cohn and Toppel of the Argonne National Laboratory devised a code for the IBM-704 which calculated reactor behavior following a step change in reactivity [5]. With some minor modifications, the code was found suitable for the

Control Data Corporation 1604 Computer.

The code is a FORTRAN program which solves the Inhour Equation for its roots by an iterative process. A LaPlace Transformation approach was used in setting up the solution. The Inhour Equation roots were then used to obtain a time solution for normalized neutron population, by means of the relationship;

$$\frac{n(t)}{n(0)} = \sum_{j=1}^{7} (A_j + B_j)\, e^{\omega_j t} + C$$

where A_j and B_j depend upon the magnitude of the step reactivity disturbance, the inhour roots, ω_j, and the magnitude of the extraneous neutron source. They are separated in the solution for ease of computation. C depends upon the reactivity step and the neutron source only. The time intervals need not be regular and were left to the choice of the programmer. See Appendix A for a discussion of the manner in which the delayed neutron effectiveness was included in this calculation.

The code presumes equilibrium of the delayed neutron emitters before the introduction of the reactivity step. A second code, devised by the same authors, permits consideration of the case where equilibrium has not been achieved.

As mentioned above, the program makes provisions for including the effect of an extraneous neutron source. The AGN-201 does have a Ra-Be source for start-up purposes. When this provision is used, the effect of the source is put in as an initial negative excess reactivity. With a source of neutrons present in a reactor, constant neutron population does not indicate criticality (zero excess reactivity). On the contrary, the reactor is subcritical by a small amount; k_{eff} is less than unity and the difficiency of neutrons is made up by the source. A convenient way

of expressing this lack of criticality is to assume an initial value of negative excess reactivity.

It was decided to exclude the source from consideration in this and other kinetic equation solutions because of the difficulty of determining an accurate value for its effect. To check on the error introduced by neglecting the external source term, an experiment was conducted. Critical rod settings were compared for two conditions; criticality at 1 watt with the source in its usual location and criticality at 1 watt with the source removed from the reactor. The difference in the two settings was so small that the experiment could not be reporduced accurately enough to detect it.

Input data for the code includes;

ϵ_{w_0} source effect (excluded in this analysis)

ρ_0 step reactivity

ℓ^* prompt neutron lifetime

λ_i delayed neutron decay constants

β_i delayed neutron fractions

time intervals

(The symbols are those used in Reference 5)

Figure 2 is a comparison of the analog time response with that obtained from the digital computer. A reactivity step disturbance of 10×10^{-4} reactivity units and a delayed neutron effectiveness of 1.14 were used in both solutions. The initial responses of the two solutions compare very well but differences appear at longer times. See Appendix A for an explaination for this behavior.

Two modifications to the analog simulation were necessary in order to compare its performance with the AGN-201 reactor. The first modification concerned the simulation of the actual reactivity disturbance of the

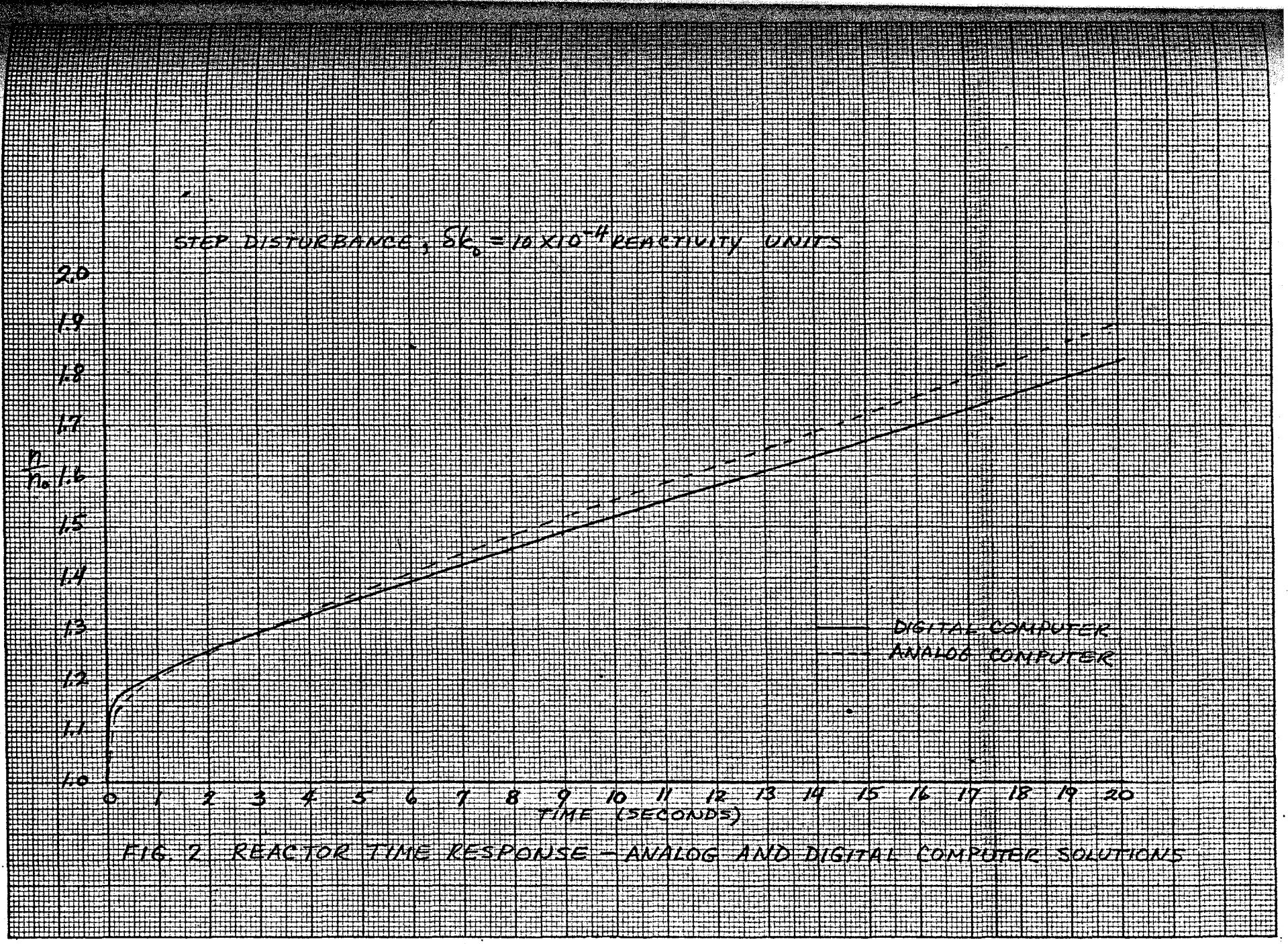

FIG. 2 REACTOR TIME RESPONSE – ANALOG AND DIGITAL COMPUTER SOLUTIONS

reactor. The reactor was disturbed by inserting a rod filled with polyethylene into the glory hole. The rod was pushed in by hand, and it was acknowledged that this resulted in a fast ramp input of finite rise time rather than a true step input. If the analog simulation was to be compared accurately with the reactor then it was necessary to disturb the analog with a fast ramp in a manner duplicating the reactor input. This was accomplished using a ramp generator.

The second modification was made necessary by the fact that the neutron detection system used in measuring the output of the reactor contained a noise filter consisting of a shunting capacitor and an input resistor to the amplifier. See Appendix C. This RC filter produced an additional time delay in the observation of the response of the reactor. The circuit components selected produced a time constant of 0.05 seconds. This filter was duplicated by a lag transfer function simulator. Fig. 3 shows the components added to the reactor simulation in order to make it comparable with the AGN-201.

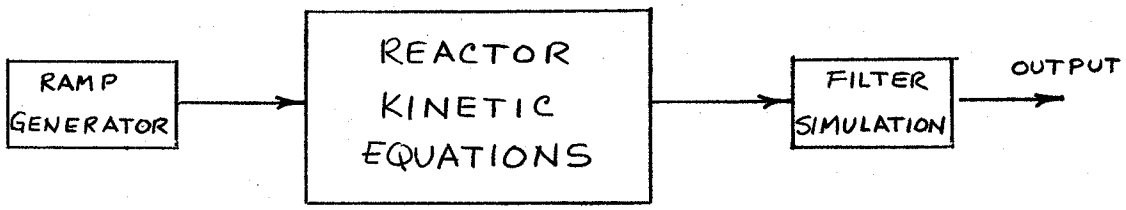

Fig. 3 Modification of analog computer to permit comparison with reactor

Details of the ramp generator and the filter simulation are contained in Appendix B.

For comparison purposes, a recording was made of the AGN-201 reactor output, following the insertion of a fast ramp-reactivity disturbance. Without changing control rod settings the time required for the reactor flux to increase by a factor of 10 was recorded. From this information, the reactor period was computed using the relationship between flux change and period,

$$\phi = \phi_0 e^{\frac{t}{T}}$$

With $\frac{\phi}{\phi_0} = 10$, the period was computed from,

$$T = \frac{t}{\log_e 10} = \frac{t}{2.3}$$

The reactivity was computed using the Inhour Equation solution for the AGN-201. A value of 15×10^{-4} was calculated. At the time this measurement was made it was recognized that this value of reactivity was too high. The period measurements were made soon after the initial fast-changing behavior of the reactor died out and the flux had settled down on an approximate exponential rise. By so doing the period was measured before all delayed neutron effects had disappeared. The resulting value of period was too low. The Inhour Equation then, gave a value of reactivity that was too high[1]. Measurements were made in this manner to avoid the effect of the negative temperature coefficient of the reactor. It takes one or two reactor periods for all the delayed neutron effects to die out after a step disturbance and the reactor to settle on a true asymptotic period. In this length of time the reactor power would have risen high

[1] In the Inhour Equation, reactivity is related to reactor period in an inverse manner. See reference (14).

enough so that the negative temperature coefficient would be introducing negative reactivity. The amount of reactivity introduced would be varying with time and attempts to compensate for it in subsequent calculations would be very difficult. It was decided to use the value of reactivity obtained in the above manner as an initial disturbance for the analog computer with the understanding that it could be legitimately reduced to obtain close agreement between the analog run and the actual reactor behavior.

On the analog computer, the value of 15×10^{-4} was used as a reactivity disturbance. Curves for reactivity rise times[1] of 0.1, 0.2, 0.5, and 1.0 seconds were obtained. These are plotted as curves one through four in Figure 4. Curve five represents the measured reactor behavior. It was decided that a rise time of 0.2 seconds best matched the reactor at low values of time. In an effort to achieve more exact matching of behavior, the reactivity input to the analog was reduced. At a value of 14.0×10^{-4} excellent agreement was obtained. This final curve was so close to other curves that it was difficult to plot. Instead isolated points are shown as crosses.

By comparison of reactivity obtained by period measurements with that obtained from critical rod settings, and from other theoretical considerations, it was estimated that the values of reactivity obtained from the reactor may be in error by as much as 3%. This does not account for the total difference shown above. It is known that β, the delayed neutron

[1]Rise time as used here refers to the time between start of insertion of the reactivity disturbance and when the full value has been applied to the reactor. See Appendix B.

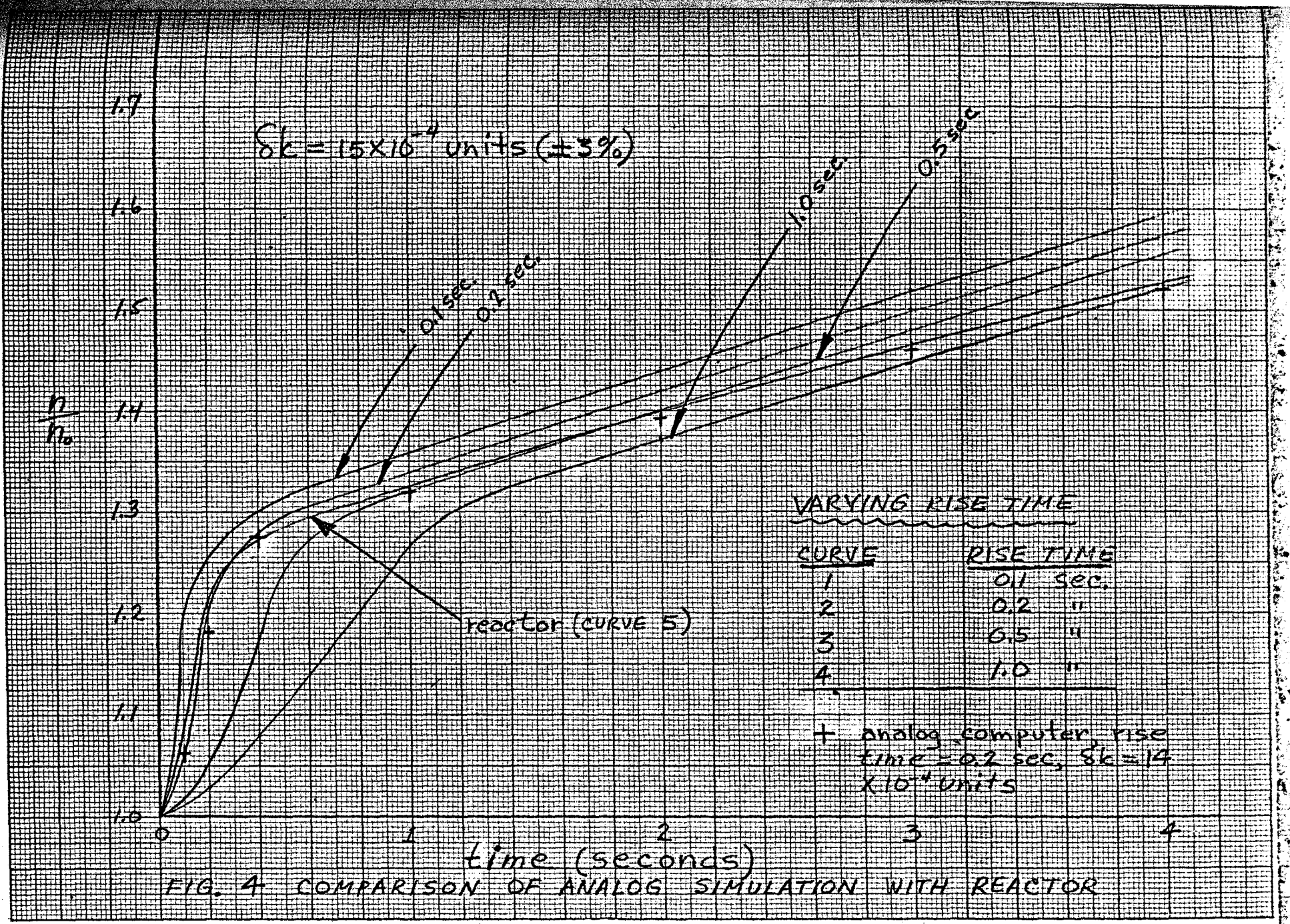

FIG. 4 COMPARISON OF ANALOG SIMULATION WITH REACTOR

effectiveness, has a sizeable effect on the behavior of a reactor at long times (after the initial fast rise). It is felt that this parameter, which was obtained unverified from Aerojet-General data, may be in error enough to account for much of the difference between the analog and reactor behavior.

While the above comparison was not analytically precise, it did lend strength to the assertion that the analog computer simulation represented the behavior of the AGN-201 with reasonable accuracy. Admittedly, the agreement was produced by a "forced fit". The adjustment of the parameters (rise time and reactivity) was logical, however, and was made in a direction permitted by theoretical considerations.

Having established the accuracy of the analog simulation, it was then used as a tool for designing and testing the automatic control system. This was accomplished by connecting the controller between amplifiers 9 and 10 as shown in Fig. 10, Appendix B. The output of amplifier 9 was applied to the control grids of tube 1 of both the UP and DOWN trigger circuits in place of V_g shown in Fig. 11, Appendix C. The relays K24 and K25 were used to operate the relay contacts shown at the input of amplifier 10.

5. Description of the Control System.

Figure 5 is a block diagram of the control system. A more detailed schematic diagram can be found in Appendix C.

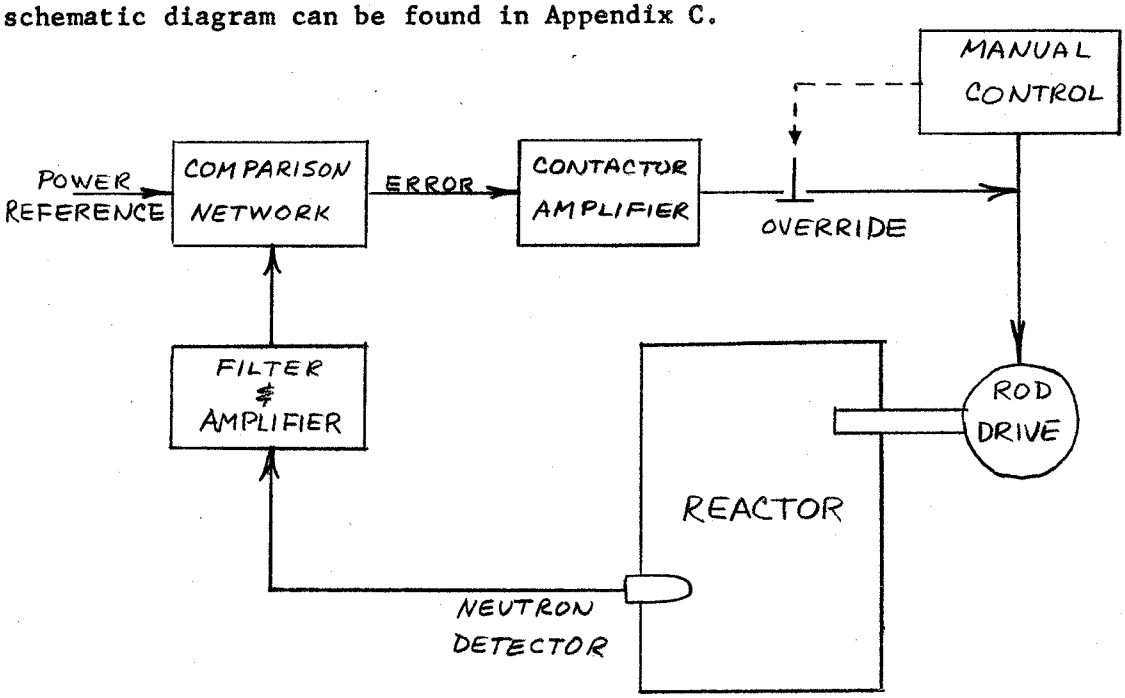

Fig. 5 Block Diagram of AFC System

The neutron detector produces an output proportional to the neutron flux of the reactor. Flux, in turn, is directly proportional to reactor power. The output of the detector is filtered, amplified and then fed to a comparison network where it is compared with a signal representing the reference power level. That is, the power level at which the AFC system is to maintain the reactor. If a difference exists between the flux and the reference signal, an error signal is generated. The contactor amplifier samples the error for size and polarity. If the error exceeds a given size the amplifier causes the rod drive mechanism to move the control rod in the appropriate direction to reduce the error signal. Since

the control system is a discontinuous type, an error signal may exist at all times if it is small enough. As long as the error stays within a designated "dead band" no control rod movement takes place. The AFC system forms a rod controlling mechanism in parallel with the manual controls of the reactor. An override is provided so that the reactor operator may disconnect the AFC system simply by manipulating the reactor control console switch for either of the control rods. The system components are described in more detail in the following paragraphs.

Neutron Detector and Signal Amplifier

A gamma-ray-compensated ionization chamber filled with boron trifluoride gas was located in one of the access ports of the AGN-201. It was supplied with a positive voltage of 250 VDC and a negative voltage of 160 VDC for compensation from an existing power supply of the reactor. Since the signal from the chamber was of the order of 10^{-9} amperes, the power supply cables and the cable returning the chamber signal were shielded throughout to reduce noise pick-up. The chamber signal was fed into a filter system consisting of a 0.1 μf capacitor and a 0.5 megohm resistor (1 megohm in parallel with the 1 megohm internal input resistance of the amplifier).

The components of this filter were chosen from noise considerations and by trial on the actual equipment. Reference [27] is an examination of the noise problems encountered in reactor instrumentation systems. It was felt that the lowest frequence of consistent noise would be 60 cycles. An initial estimate of filter parameters was made by assuming a 40 db attenuation of 60 cycle noise. A Bode plot gave a time constant of 0.267 sec. (breakpoint frequency of 3.75 rad./sec.) In order to reduce

the time delay of signal changes, the time constant was decreased experimentally by decreasing the capacitor and resistor values with the neutron chamber and a recorder in operation. A satisfactory arrangement was achieved at a time constant of 0.05 sec. (Breakpoint frequency of 20 rad./sec.) This value of time constant had a minor effect upon chamber signal changes but still accomplished adequate noise filtering. This value might have been decreased still further, but at 0.01 seconds too much noise was being passed. No further effort was made toward finding optimum filter parameters.

Amplification of the chamber signal was accomplished using a low-drift, high-gain amplifier, Brush Model BL-550.

Comparison Network

Discounting the complicated initial behavior of a reactor immediately after a step reactivity disturbance, the reactor response, after a sufficiently long period of time, is basically of the exponential type characterized by the equation

$$n = n_o e^{\frac{t}{T}} \qquad (14)$$

We have seen that the reactor period, T, is related in an inverse manner to reactivity through the Inhour Equation. Thus,

$$\frac{n}{n_o} = e^{\frac{t}{T}} \propto \delta k$$

For a given reactivity disturbance, n/n_o is the same value, at any given time, regardless of the power level at which the disturbance occurred. In reactor control, error determination is not a matter of subtracting a reference value from a measured quantity. Rather it is the division of the measured quantity by the reference and the determination of the deviation of this normalized quantity from unity. Thus,

$$\frac{n}{n_o} = \frac{n_o + \Delta n}{n_o} = 1 + \frac{\Delta n}{n_o}$$

A comparison network was chosen that would perform this division by n_o and would permit n_o to be varied according to the power level desired. [23]. Referring to Fig. 6,

$$V_g = \frac{V_n}{1 + \frac{PD}{R}}$$

by the principle of voltage division, provided the current to the trigger circuit grids is kept very small.

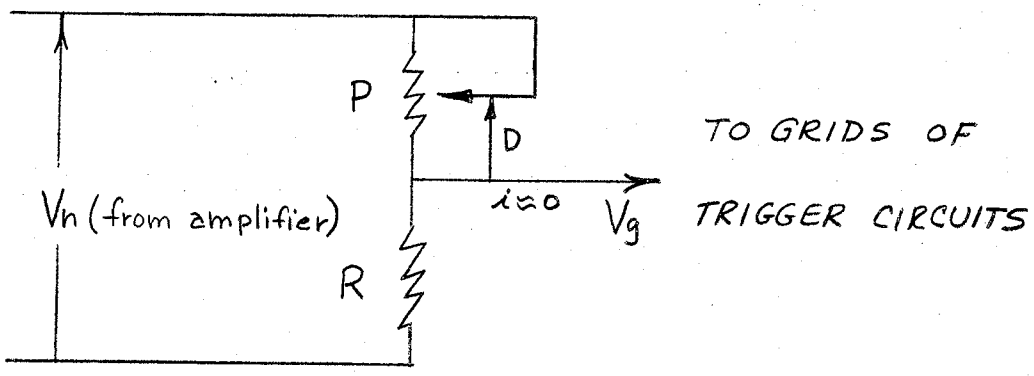

Fig. 6 Comparison Network

It is convenient for the circuitry that follows (Trigger circuits) to have V_g represent a base voltage plus an error. A base voltage of 10 volts was chosen.

$$V_g = 10 + V_e$$

then

$$V_e = V_g - 10 = \frac{V_n}{1 + \frac{PD}{R}} - 10$$

$$= \frac{V_n - 10\left(1 + \frac{PD}{R}\right)}{1 + PD/R}$$

Let V_o, the reference voltage, equal $10(1 + PD/R)$, then,

$$V_e = \frac{V_n - V_o}{\frac{V_o}{10}} = \frac{10(V_n - V_o)}{V_o}$$

If V_n represents n, and V_o represents n_o, then the output error voltage is of the required form

$$V_e = \frac{10(V_n - V_o)}{V_o} \Rightarrow \frac{K(n-n_o)}{n_o} = K\frac{\Delta n}{n_o}$$

The value of P/R was chosen to be 2. The output voltage, V_g, then becomes 10 volts plus or minus an error proportional to $\Delta n/n_o$. The potentiometer setting, D, becomes the variable parameter that determines V_o, the reference voltage representing the desired power level.

$$V_o = 10(1+2D)$$

This analysis presumes that V_n never goes below 10 volts or above 30 volts (D = 1 gives V_o = 30 volts). This was easily arranged by the scale changes on the amplifier.

Contactor Amplifier

Two Schmitt Trigger Circuits arranged as shown in Fig. 11, Appendix C operate relays and perform the function of measuring the error and initiating control rod movement when required [21]. The trigger circuit, shown in Fig. 7., is a network with two stable operating conditions; one when V_g is below the voltage of the grid[1] of tube 2, the second when V_g is above grid of tube 2. As V_g increases and approaches the voltage of the grid of tube 2, tube 1 is cut off, R5 having been chosen so that the cathode voltage is high enough to permit this action. Tube 2 is above cutoff and is conducting. The relay is in the energized condition. As V_g approaches a value slightly below cathode voltage, tube 1 begins to conduct a small amount. This reduces the voltage at the plate of T1 and, through voltage divider action, reduces the grid voltage of T2. This action starts to cut off T2 which reduces voltage across R5. As a

[1]The term grid refers to the control grid, in this report.

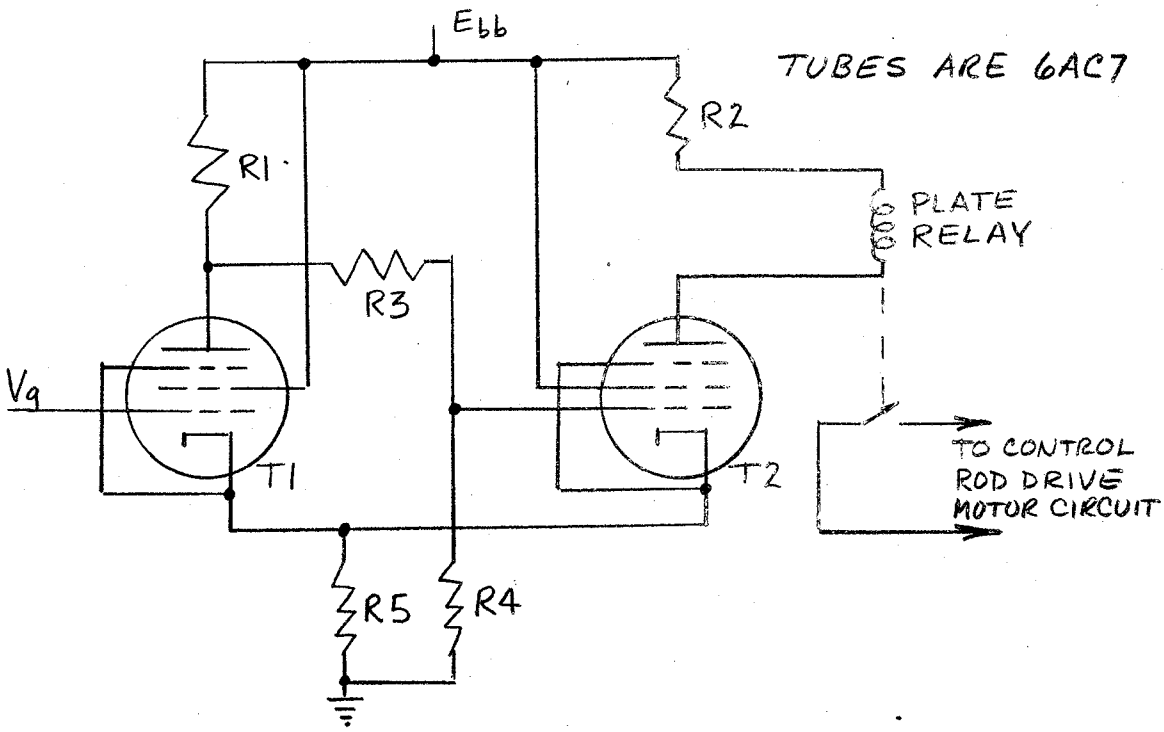

Fig. 7 Schmitt Trigger Circuit

result the cathode to grid voltage of T1 reduces and the cycle repeats itself. The action is cumulative and the trigger changes to the new stable condition with T1 conducting and T2 cut off, thereby de-energizing the relay. R5 and R4 are chosen so that the trigger point is just above 10 volts and so that the trigger action is as sharp as possible. R1 and R2 are chosen by plate current considerations and R3 was determined by voltage division requirements. E_{bb} was approximately 150 volts. The resulting effect is that when V_g rises a small amount above 10 volts the relay changes condition (de-energizes). This relay action can be used to start control rod motion in such a direction that V_g returns to 10 volts. A second circuit, operating above the trigger point can be used to detect negative error. In this case, as V_g goes below 10 volts tube 2 starts to conduct and the relay energizes. The two relays, one responding to positive error, the other to negative error are used to close switches in the power supply circuit of the control rod drive motor to move the

rod in the required direction. Figure 12, Appendix C shows the connections to the existing AGN-201 motor control circuits.

6. Performance of the Control System.

When installed on the AGN-201, the automatic control system proved to be a simple, effective device which met most of the design criteria. The requirement that accuracy of control be within 1% proved to be unrealistic for a discontinuous system of this type on this reactor. The difficulty was not so much in the inability of the system to respond with the necessary sensitivity but rather in the achievement of a proper compromise between accuracy and control rod movement. When an attempt was made to reduce the controller dead band to 1% either side of the desired power level, the control rod remained in virtually continuous operation. The resulting wear on the mechanical parts and the heating of the motor by continual starting was felt to be unacceptable. By widening the dead band to about $\pm$ 3% satisfactory operation was achieved.

Fig. 8 shows a comparison of the analog simulation performance with the performance of the AGN-201 under essentially the same conditions (same reactivity disturbance and rod correction rate). A step (fast ramp) reactivity disturbance of about 10×10^{-4} units was used. A control rod correction rate of 0.860×10^{-4} units/sec., from the fine rod, fast speed, was used in the reactor and was simulated on the analog computer. For purposes of comparison, the following two standards for measuring performance are defined;

Delay Time - The elapsed time between insertion of disturbance and the time when the curve first returns to the dead band.

Maximum Power Rise - The normalized rise of neutron flux. That is, the peak value divided by the initial value.

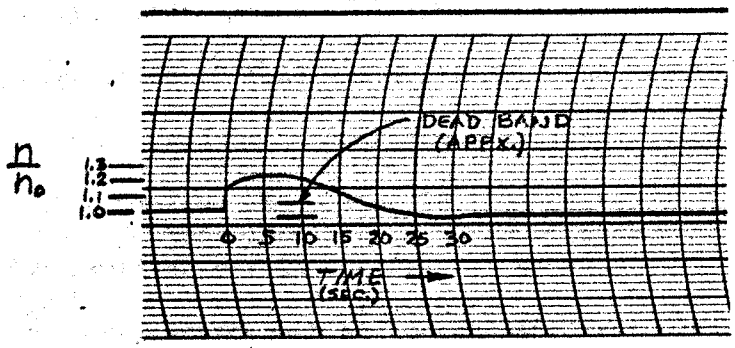

(a) ANALOG

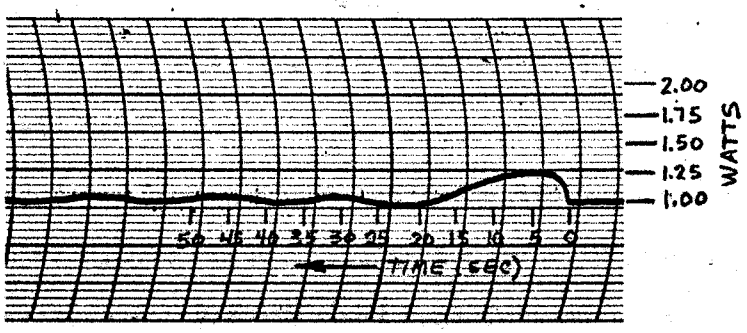

(b) REACTOR

$\delta k_D = 10 \times 10^{-4}$

δk_R RATE $= 0.860 \times 10^{-4}$ δk_R/SEC.

FIG 8 COMPARASON OF ANALOG SIMULATION WITH AGN-201 REACTOR WITH CONTROLLER ATTACHED

Curve (a), from the analog computer, shows normalized neutron density (n/n_o). The initial value is unity. A delay time of 18 seconds and a maximum power rise of 1.23 was observed. The reactor behavior, curve (b) shows 15 seconds and 1.25 for these quantities. The dead band in curve (a) extends from line 16 to line 18. In Curve (b) it is readily noticeable. The oscillations in the reactor behavior and the lack of them in the analog curve points out an interesting fact observed in this study. It was found that it was not possible to duplicate the behavior of the analog trace within the dead band. While the analog behavior from one run to another was generally the same, small differences in the mechanical action of the relays in subsequent runs made the oscillations uneven and different from run to run. In some cases (curve (a) is an example) the relay action was such that the trace returned to the dead band and remained relatively level for a long period of time before control rod action was called for. During other runs, the analog remained in oscillation as the reactor did in curve (b). By the same token, in some of the reactor runs, the flux entered the dead band in such a manner that no oscillations occurred for a time. This was probably due to fortuitous action of the relay and some coasting of the rod after the control circuit was opened, with the result that the reactor was left very close to criticality when the controller action stopped. Whenever this happens it is by chance since the on-off action of the controller is not expected to provide exactly the correct amount of reactivity correction.

The small differences between the two curves, as well as all differences observed between the analog computer and the reactor during this study can be attributed to uncertainties and inaccuracies in several

quantities. They are summarized below.

1. Uncertainties in the amount of reactivity disturbance used in the reactor.
2. The estimation of the control rod drive mechanism time constants.
3. The estimation, done by forced fit, of the rise time of reactivity into the reactor.
4. The use of 1.14 for γ with no precise knowledge of the derivation of that quantity and thus its accuracy.
5. Uncertainty in the value of neutron lifetime in this reactor.
6. The inaccuracies inherent in any simulation. The fact that the behavior of a reactor is represented by a set of differential equations is a mathematic approximation, or model, of a physical system.

In the light of the above known limitations, it is felt that excellent agreement was achieved between predicted reactor behavior and the performance of the reactor. The design procedure employed in this investigation appears to be an accurate and practical experimental method of designing control systems.

Fig. 9 curves were obtained from a recorder attached to one of the neutron channels of the AGN-201. Fig. 9(a) shows the behavior of the reactor when a reactivity correction rate of 0.282×10^{-4} was employed (fine rod, slow speed). This run was made at 0.1 watts. Note the typical behavior of a discontinuous control system before and after the disturbance. The set power level of 0.1 watts is located on the arbitrary

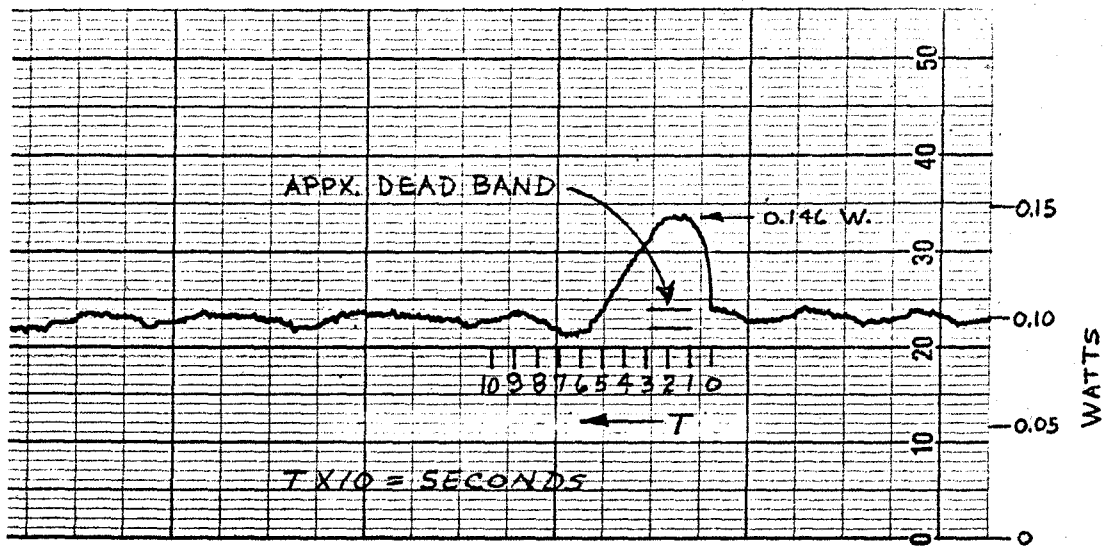

(a) $\delta k_D = 10 \times 10^{-4}$

δk_R RATE $= 0.282 \times 10^{-4}\ \delta k_R/\text{SEC.}$

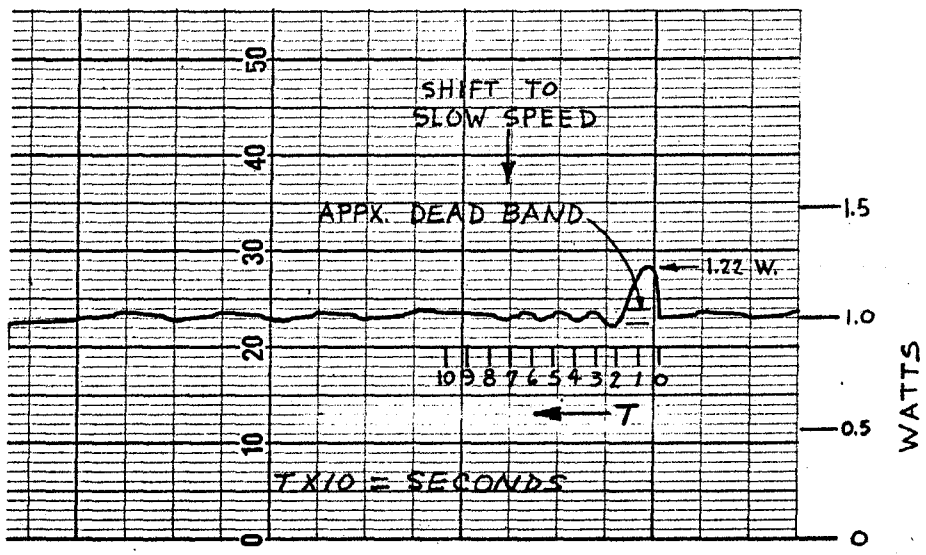

(b) $\delta k_D = 10 \times 10^{-4}$

δk_R RATE $= 0.860 \times 10^{-4}\ \delta k_R/\text{SEC}$

$= 0.282 \times 10^{-4}\ \delta k_R/\text{SEC}$ AFTER 70 SEC.

FIG. 9 TIME BEHAVIOR OF AGN-201 UNDER CONTROL OF AUTOMATIC FLUX CONTROL SYSTEM

scale at about 23. The dead band extends from 22 to 24. This curve shows a delay time of 50 seconds and a maximum power rise of 1.47. Curve (b), taken at 1 watt with the same input shows better performance of the control system. In this run, fine rod, fast speed was used initially, to obtain fast error correction, then the rod speed was manually shifted to slow after about 70 seconds to reduce the oscillation of the reactor within the dead band. Curve (b) was the best performance of the control system observed during this investigation. Note that the dead band is about the same percentage of the reference level in the two cases. A scale change has occurred on the neutron channel between the two curves. In curve (a) the dead band is about 0.008 watts, which represents 8% of the reference, 0.1 watts. In curve (b) the dead band is about 0.06 watts, which is 6% of the reference, 1 watt. The closeness of these two percentages indicated the successful division by n_o discussed in Section 5 in regard to the design of the comparison network. The slightly smaller value for curve (b) can be attributed to the reduced noise level at 1 watt operation. The signal in curve (a), for 0.1 watts, is comparatively noisy so the curve appears to have a larger dead band.

7. Improvement of the Control System.

The major difficulty experienced in the operation of the control system was in the adjustment of the trigger circuits employed to actuate the relays. Referring to Fig. 11, Appendix C, the interaction between R4 and R5 in achieving fast trigger action and low hysteresis[1] is difficult to define precisely. The circuit parameters were chosen largely by trial. While satisfactory performance was achieved and the circuits were stable once adjustments were made, the adjusting procedure was time consuming and had to be made before each series of runs.

It is felt that more investigation is necessary into the behavior of the Schmitt Trigger Circuit in order to improve its performance in an application such as that made in this work. No reference was found, for example, on the effect of an inductive loading, such as the control relays, in the plate circuit of tube 2 of the trigger.

Further investigation may show the desirability of using variable control rod drive, possibly adjusted by tachometer feedback. There are other controls that could be added to make control action smoother and more precise. The addition of these devices must be weighed against cost and additional complexity. This is particularly true when the control system is for a low power, low cost research reactor such as the AGN-201.

[1]Hysteresis refers to the fact that trigger action does not occur at the same value of V_g when the signal is increasing as it does when the signal is decreasing.

APPENDIX A

DELAYED NEUTRON EFFECTIVENESS

The delayed neutrons produced in the fission of U^{235} are emitted with an average energy of 0.515 MEV [8]. The prompt neutrons, on the other hand, have an average energy of about 2 MEV at emission. Due to their lower energy, the delayed neutrons are less likely to leak out of the reactor during the slowing down process. This "less liklihood of leaking out" can be expressed as an increased effectiveness of the delayed neutrons in producing fissions. A greater percentage of the delayed neutrons will reach thermal energy and cause further fissions than will their prompt counterparts. This is the reason for including a parameter of this type in reactor kinetic investigations.

The average delayed neutron effectiveness $\gamma' = \frac{1}{\beta} \sum_{i}^{k} \beta_i \gamma'_i$, is usually greater than unity[1]. In small, water-moderated reactors, this parameter may exceed unity by as much as 25% [12]. In work of low precision, its value is usually taken as one. Actually, there is an effectiveness for each of the delayed neutron groups. The individual values are difficult to determine, however, so an average quantity, for the aggregate, is generally used.

The method of including γ' in kinetic equations varies, superficially, in the literature. The fundamental approach, however, is the same. Handler [15] defines γ' mathematically as shown in Section 3. To be consistent, he also redefines k_{eff} to account for the different behavior

[1] Keepin [19] states that the parameter may be less than unity in a fast Pu - metal reactor.

of the prompt and delayed neutrons. Gwin [22] has a similar expression for k_{eff}.

$$k_{eff} = (1-\beta)\, k_{eff,prompt} + \sum_{1}^{6} \beta_i\, k_{eff,i\,(delayed)}$$

$$= \frac{(1-\beta)\, k_\infty e^{-B^2 T_p}}{1+L^2B^2} + \sum_{1}^{6} \beta_i\, k_{\infty,i}\, e^{-B^2 T_{d,i}}$$

$$= \frac{k_\infty e^{-B^2 T_p}}{1+L^2B^2} \left\{ (1-\beta) + \sum_{1}^{6} \beta_i \gamma_i \right\} \quad \text{since } k_\infty = k_{\infty,i}$$

let $$\Gamma = 1 - \beta + \sum_{1}^{6} \beta_i \gamma_i$$

then $$k_{eff} = \frac{k_\infty e^{-B^2 T_p}}{1+L^2B^2}\, \Gamma$$

This method of accounting for γ is entirely equivalent to those found in the literature [6] [26] . They all lead to the same time behavior of thermal neutrons in a reactor. This investigator has chosen to incorporate the effect of delayed neutrons in the manner shown in Section 3. This approach permits a logical, mathematical development of the parameter γ . In the digital computer solution, it was convenient to use a modifying factor for β as did Goertzel [26] because of the particular form of the mathematical expressions used and because the FORTRAN code could be most easily modified by changing the β values. In accounting for delayed neutron effectiveness by the method of modifying β , some other changes in the kinetic equations are also required in order to make the equations agree mathematically with the Handler development. Unfortunately, without making major modifications in the code, these changes could not be included. This is the reason that the two curves of Fig. 2 show large differences at long time values. The digital solution does not accurately include the effects of delayed neutrons, and

thus is assumed to be in error. The direction of the error is not known. The digital solution does provide an approximate comparison for the analog for purposes of checking the accuracy of simulation, particularly at low time values.

APPENDIX B

ANALOG COMPUTER PARAMETERS

Pot	Mathematical Expression	Value	Pot Setting	Amplifier	R input	Feedback
1	$\frac{\lambda_1}{a}$	.0124	.0124	1	1 M	1 μf
2	$\frac{\lambda_2}{a}$	.0305	.0305	2	1 M	1 μf
3	$\frac{\lambda_3}{a}$	.1114	.1114	3	1 M	1 μf
4	$\frac{\lambda_4}{a}$	.3013	.3013	4	1 M	1 μf
5	$\frac{\lambda_5}{a}$	1.136	.1136	5	0.1 M	1 μf
6	$\frac{\lambda_6}{a}$	3.013	.3013	6	0.1 M	1 μf
7	$\frac{b\gamma\beta_1}{g\beta}$	.00374	.0374	11	1 M	0.1 M
8	$\frac{b\gamma\beta_2}{g\beta}$	.02480	.2480	11	1 M	0.1 M
9	$\frac{b\gamma\beta_3}{g\beta}$	.02235	.2235	11	1 M	0.1 M
10	$\frac{b\gamma\beta_4}{g\beta}$	.04490	.4490	12	1 M	0.1 M
11	$\frac{b\gamma\beta_5}{g\beta}$	.01311	.1311	12	1 M	0.1 M
12	$\frac{b\gamma\beta_6}{g\beta}$	.00475	.0475	12	1 M	0.1 M
13	$\frac{g\lambda_1}{ab}\left(\frac{1}{10}\right)$*	.0124	.0124	1	1 M	1 μf
14	$\frac{g\lambda_2}{ab}\left(\frac{1}{10}\right)$	.0305	.0305	2	1 M	1 μf
15	$\frac{g\lambda_3}{ab}\left(\frac{1}{10}\right)$	.1114	.1114	3	1 M	1 μf
16	$\frac{g\lambda_4}{ab}\left(\frac{1}{10}\right)$	.3013	.3013	4	1 M	1 μf
17	$\frac{g\lambda_5}{ab}\left(\frac{1}{10}\right)$	1.136	.1136	5	0.1 M	1 μf
18	$\frac{g\lambda_6}{ab}\left(\frac{1}{10}\right)$	3.013	.3013	6	0.1 M	1 μf
19	$\frac{g\lambda_1\beta}{ea}(100)$**	.0400	.0400	1	1 M	1 μf
20	$\frac{g\lambda_2\beta}{ea}(100)$	.0981	.0981	2	1 M	1 μf
21	$\frac{g\lambda_3\beta}{ea}(100)$	.3580	.3580	3	1 M	1 μf
22	$\frac{g\lambda_4\beta}{ea}(100)$	.9685	.9685	4	1 M	1 μf
23	$\frac{g\lambda_5\beta}{ea}(100)$	3.653	.3653	5	0.1 M	1 μf

Pot	Mathematical Expression	Value	Pot Setting	Amplifier	R input	Feedback
24	$\frac{g\lambda_6\beta}{ea}(100)$	9.685	.9685	6	0.1 M	1 μf
25	$\frac{g\lambda_1\beta}{eab}(100)^{***}$	.0040	.0040	1	1 M	1 μf
26	$\frac{g\lambda_2\beta}{eab}(100)$	.0098	.0098	2	1 M	1 μf
27	$\frac{g\lambda_3\beta}{eab}(100)$	.0358	.0358	3	1 M	1 μf
28	$\frac{g\lambda_4\beta}{eab}(100)$	.0968	.0968	4	1 M	1 μf
29	$\frac{g\lambda_5\beta}{eab}(100)$	.3653	.3653	5	1 M	1 μf
30	$\frac{g\lambda_6\beta}{eab}(100)$	.9685	.9685	6	1 M	1 μf
31	$\frac{b(1-\beta)}{e}$	.4968	.4968	13	1 M	
32	$\gamma\left(\frac{1}{10}\right)^{*}$	.1140	.1140	13	1 M	
33	$\frac{1-\beta}{e}$	.0497	.0497	13	1 M	
34	$\frac{10\,la}{\beta}$	.0638	.0638	13	1 M	
35	$\frac{e}{b}\delta k_0$	See pg 45				
36	e_1	See pg 45				
37	$+e_r$	See pg 47				
38	$-e_r$	See pg 47				
39	n_o	10^v				

* $10\Delta n_1'$ is input to potentiometers

** $\frac{1}{100}\delta k_1'$ is input to potentiometers

*** $\frac{1}{100}\Delta n_1'\,\delta k_1'$ is input to potentiometers

PARAMETERS FOR REMAINING AMPLIFIERS

AMPLIFIER No.	USE	Input	R in	Feedback
7	INT	$(\frac{1}{10})\frac{d\Delta n'_1}{dt}$	0.1 M	0.1 μf
8	INT	e_1	1.0 M	1 μf
9	LAG	n'_1	0.5 M	0.1 μf
				0.5 M
10	INT	e_r	1 M	1 μf
14	INV	$10\Delta n'_1$	1 M	1 M
15	INV	$10\Delta n'_1$	1 M	1 M
16	INV	$\delta k'_1$	0.1 M	1 M
17	INV	$\delta k'_1\Delta n'_1$	1 M	1 M
18	INV	$\delta k'_1\Delta n'_1$	1 M	0.1 M
19	INV	$\frac{1}{10}\delta k'_1\Delta n'_1$	1 M	0.1 M
20	INV	Pot 35	1 M	1 M
21	SUM	$\delta k'_{1D}$	1 M	1 M
		$\delta k'_{1R}$	1 M	
22	INV	$\delta k'_1$	1 M	1 M
23	INV	$\delta k'_1$	1 M	0.1 M
24	INV	$\frac{1}{10}\delta k'_1$	1 M	0.1 M
25	SUM	$10\Delta n'_1$	1 M	0.1 M
		n'_0	0.1 M	0.1 M
26	LAG	$\delta k'_{1R}$	1 M	1 M
				0.1 μf

Ramp Generator

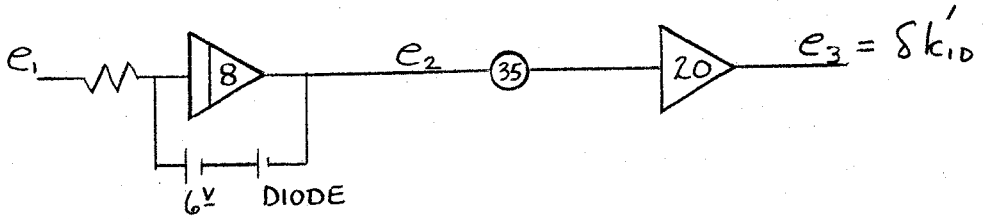

It is required that the generator input a specified amount of reactivity in time t seconds.

$$\dot{e}_3 = \frac{e_D}{t} \qquad \text{where} \qquad e_D = \frac{e}{\beta}\delta k_D$$

$$e_{3,MAX} = e_D$$

The output of integrator 8 becomes,

$$\dot{e}_2 = \frac{e_D}{a_{35}t}$$

$$e_{2,MAX} = \frac{e_D}{a_{35}}$$

Let the characteristics of the diode be such that with a bias of 6^V as shown, the diode cuts off the integrator output at voltage e_c (close to 6^V). Then,

$$e_{2,MAX} = \frac{e_D}{a_{35}} = e_c$$

and

$$a_{35} = \frac{e_D}{e_c}$$

We know that

$$e_1 = \dot{e}_2 = \frac{e_D}{a_{35}t} = \frac{e_c}{t}$$

Given the values of e_c, e_D and t, solution for a_{35} and e_1 can be obtained, giving the desired reactivity input in the given rise time interval. For t = 0.2 sec. and $\delta k_d = 10 \times 10^{-4}$, the output of inverter amplifier 19 has the following shape.

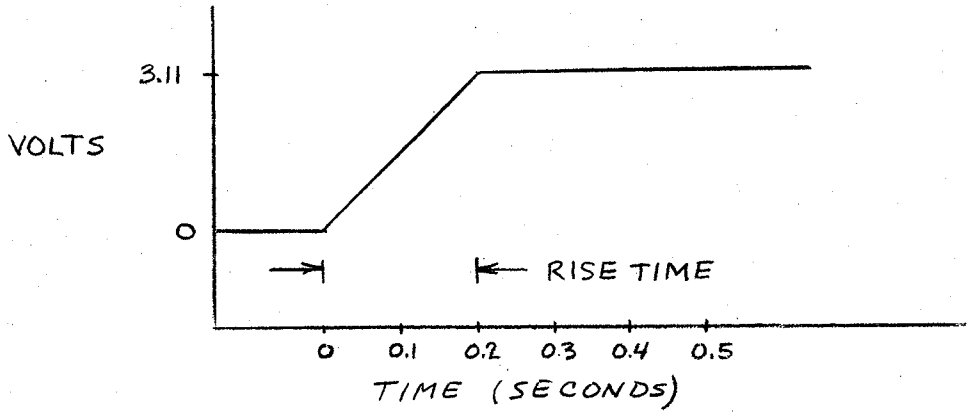

Filter Simulation

It is desired to simulate the transfer function,

$$G(s) = \frac{1}{RCS+1}$$

$$G(s) = \frac{1}{.05S+1}$$

where $R = 0.5\ M$

$C = 0.1\ \mu f$

The following analog computer set up will provide this simulation

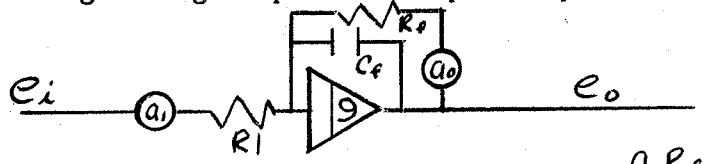

$$\frac{e_o}{e_i} = \frac{\frac{a_1 R_f}{a_0 R_1}}{\frac{C_f R_f}{a_0} S + 1}$$

thus $\frac{a_1 R_f}{a_0 R_1} = 1$

and $\frac{C_f R_f}{a_0} = .05$

Let $a_1 = 1$

$a_o = 1$

$R_f = 0.5$ M

$R_1 = 0.5$ M

$C_f = 0.1 \mu f$

Control Rod Simulation

Simulation of the rod drive transfer function, $\frac{1}{S(0.1S+1)}$ was accomplished by use of an integrator and a lag transfer function simulation identical to the filter simulation but with different parameters.

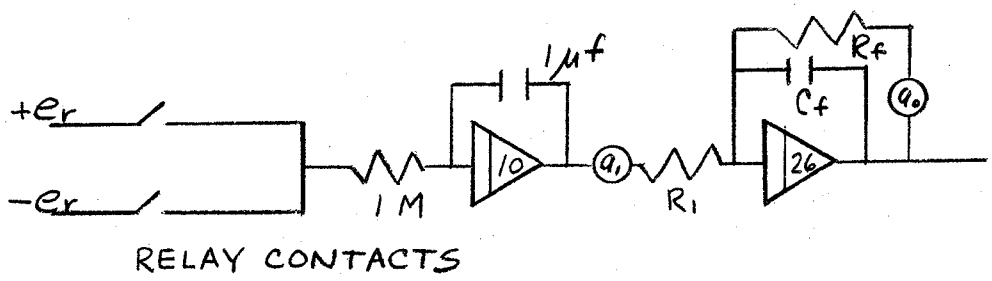

$R_1 = 1\ M$

$R_f = 1\ M$

$a_1 = 1$

$a_o = 1$

$C_f = 0.1\ \mu f$

Delayed Neutron and Reactor Parameters.

The delayed neutron parameters used in this analysis were those due to Keepin and others [20].

λ_1	= 0.0124	β_1	= 0.000211
λ_2	= 0.0305	β_2	= 0.00141
λ_3	= 0.112	β_3	= 0.00126
λ_4	= 0.301	β_4	= 0.00254
λ_5	= 1.14	β_5	= 0.00740
λ_6	= 3.01	β_6	= 0.00268

$\beta = 0.00643$

The reactor parameters were obtained from Aerojet-General [1] and Cooke [8].

$\ell = 4.1 \times 10^{-5}$ sec.

$\gamma = 1.14$

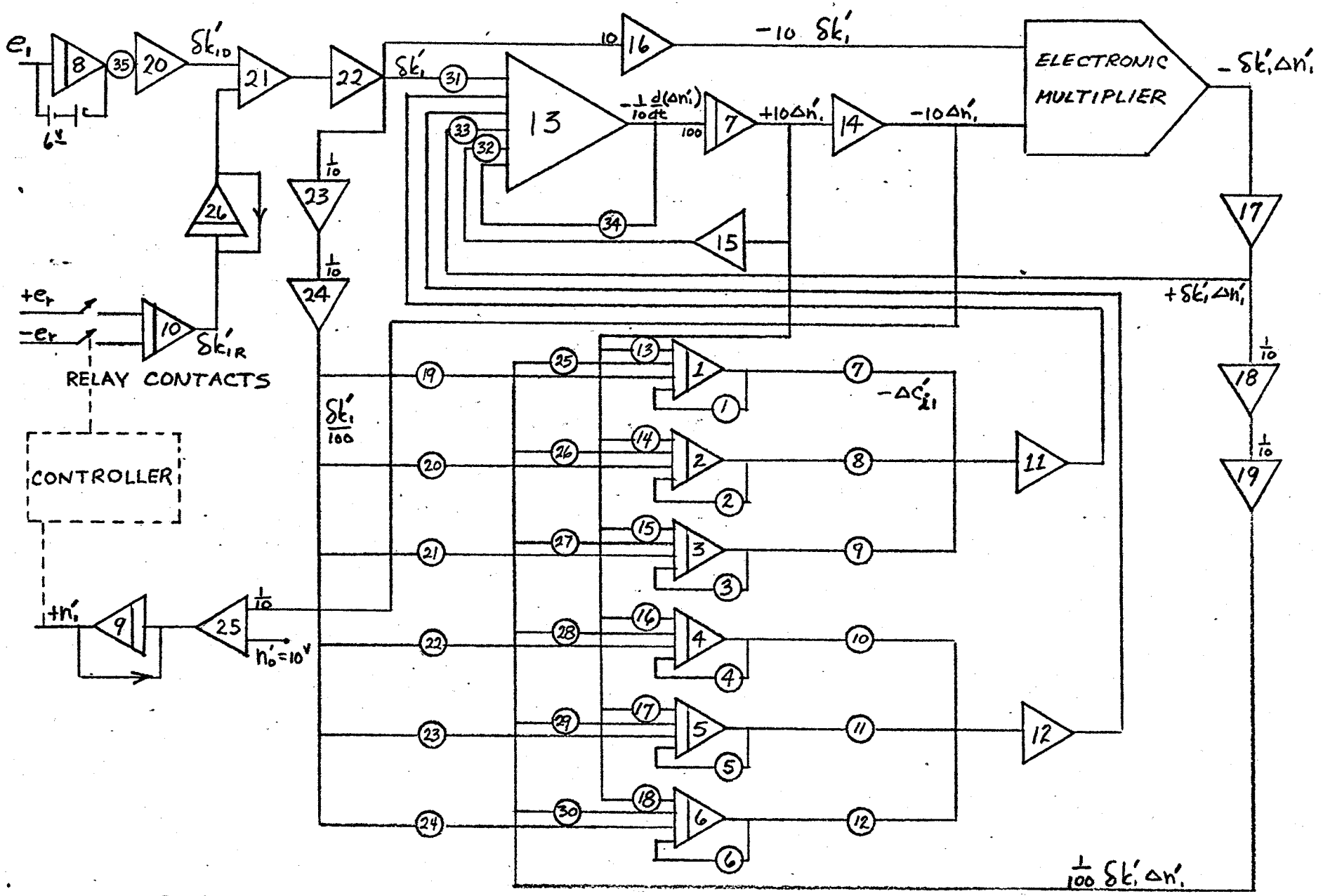

FIG. 10 SCHEMATIC OF ANALOG COMPUTER SIMULATION

APPENDIX C

AUTOMATIC FLUX CONTROL SYSTEM SCHEMATICS

Figures 11 and 12 are schematics of the trigger circuits and motor control circuits for the automatic flux control system. The following notes will aid in their understanding.

A. Fig. 11

1. Resistor values used in this study were:

DOWN and UP

R1 = 2.2 K

R2 = 2.7 K

R3 = 100 K

DOWN

R4 = 9.4 K (adjustable)

R5 = 680 (adjustable)

UP

R4 = 8.2 K (adjustable)

R5 = 400 (adjustable)

E_{bb} = 140 volts

2. K22 and K23 were sensitive relays designed for pull-in at about 5 ma. The trigger circuits were found to have best operation with plate current at about 15 ma. The variable resistor shunting the relays were used to by-pass the excess current.

3. Being sensitive relays, K22 and K23 had only one set of contacts. They were used to control relays K24 and K25 which had the necessary number of contacts to perform switching in the motor control circuit.

4. The diodes around K24 and K25 were found necessary to reduce arcing when these relay coil circuits were opened.

5. The following adjustment procedure, used for a particular set of tubes, is offered for reference. The voltages will be different for other tubes.

   a. Adjust E_{bb} to 136 volts.

   b. Adjust V_g to 10.0 volts with external power supply.

   c. DOWN

      (1) AdjustR4 until grid, tube 2 reads 10.0 volts.

      (2) Adjust R5 until cathode reads 11.6 volts.

   d. UP

      (1) Adjust R4 until grid, tube 2 reads 7.7 volts.

      (2) Adjust R5 until cathode reads 10.4 volts.

The above voltages are with respect to - E_{bb}, at the negative of the amplifier output.

6. P stands for a 50 K potentiometer. R is a 25 K resistor. D refers to the potentiometer setting ($0 \leq D \leq 1$).

B. Fig. 12.

1. The wiring additions are those circuits showing contacts from K20, K21, K24 and K25. The other circuits were original circuits on the AGN-201.

2. The existing relays have the following function

   a. K16 - Energized by lower limit switch, fine control rod .

   b. K17 - upper limit switch

   c. K18 - Energizes when a scram occurs in order to return all rod carriages to the down position.

3. K20 is a small SPDT 6 volts relay

4. K21 is a 6PDT telephone type relay rated at 110 volts.

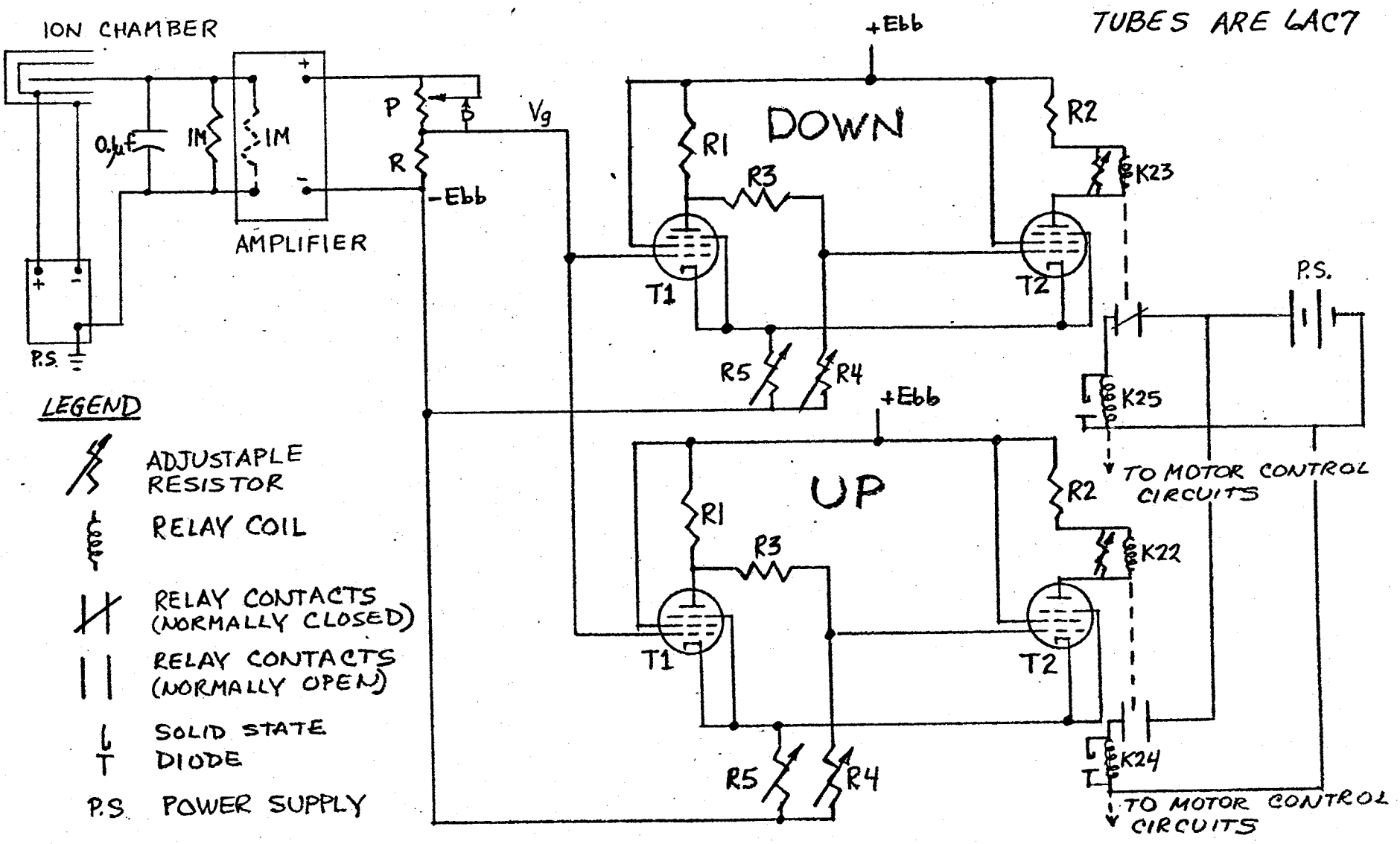

FIG. 11 AUTOMATIC FLUX CONTROL SYSTEM - TRIGGER CIRCUITS

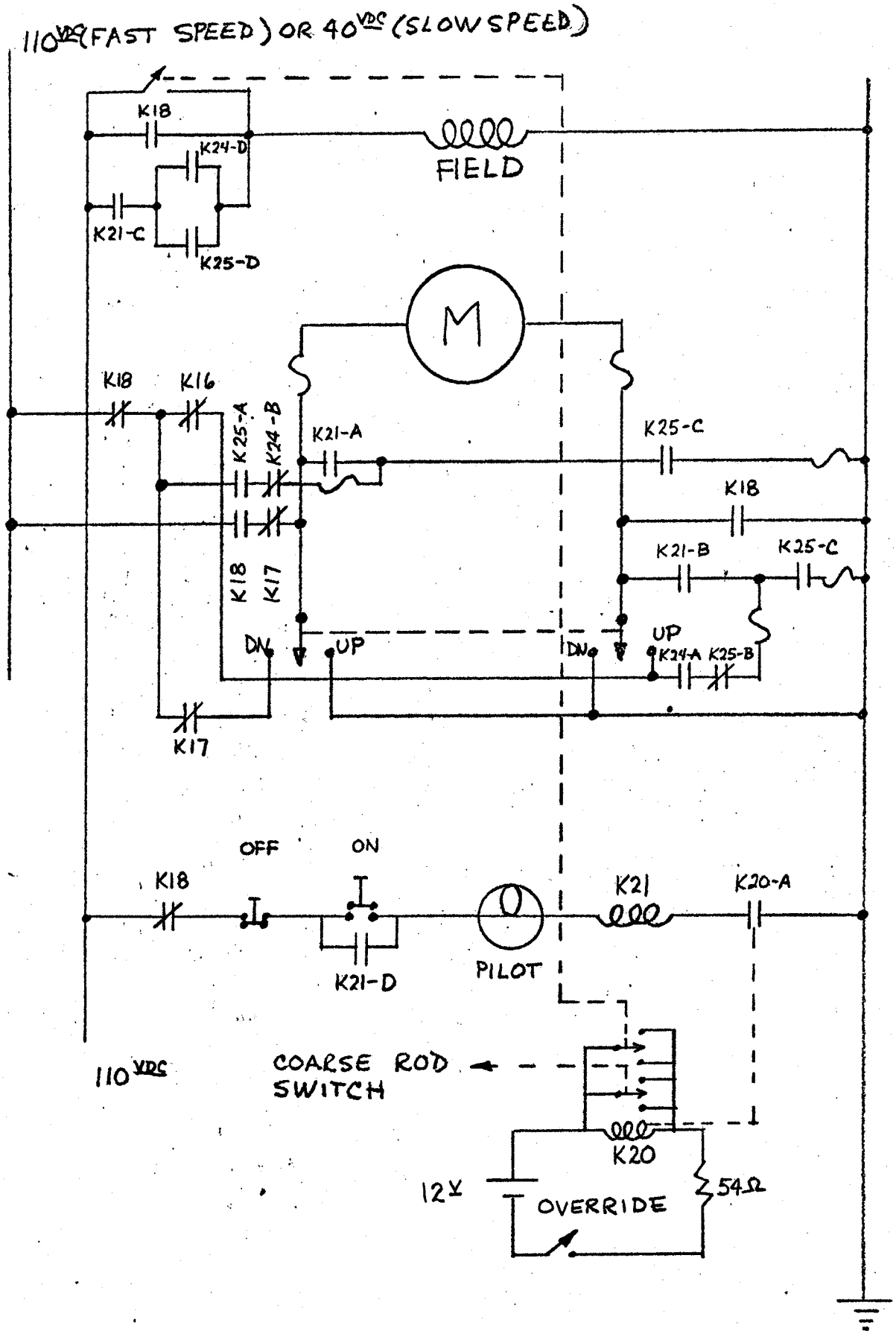

FIG. 12 AUTOMATIC FLUX CONTROL SYSTEM - FINE ROD MOTOR CONTROL CIRCUITS

BIBLIOGRAPHY

1. Aerojet-General Nucleonics. A Summary of Experimental Investigations of the AGN 201 by M. M. Harvey and others. AGN report 22. June 10, 1957.

2. Argonne National Laboratory. Dynamics Analysis of Natural Circulation Boiling Water Power Reactors by E. S. Beckjord. March, 1958. Report No. ANL 5799.

3. Argonne National Laboratory. Analogue Computer Solution of the Nonlinear Reaction Kinetic Equations by L. T. Bryant and N. F. Morehouse, Jr., July, 1959. Report No. ANL-6027.

4. Argonne National Laboratory. Argonaut Automatic Flux Controller Design Report by A. Gerba, Jr., January, 1960. Report No. ANL-6110.

5. Argonne National Laboratory. IBM-704 Codes for Reactivity Step Calculations (RE-216 and RE-135) by C. E. Cohn and B. J. Toppel. March, 1960. Report No. ANL-6134.

6. Argonne National Laboratory. The Reactor Kinetics of the Transient Reactor Test Facility (TREAT), by Okrent and others. September, 1960. Report No. ANL-6174.

7. Biehl, A. T. and others. Compact, Low-Cost Reactor. Nucleonics, V. 14. September, 1956: 100-103.

8. Cooke, W. B. H., Predicted Behaviour of the AGN 201 Reactor at High Power Levels. Master's Thesis, The United States Naval Postgraduate School, Monterey, California, 1961.

9. Chestnut, H. and R. W. Mayer. Servomechanisms and Regulating System Design. John Wiley and Sons, Inc., 1951.

10. D'Azzo, J. J., and C. H. Houpis. Feedback Control System Analysis and Synthesis. McGraw-Hill, 1960.

11. Donner Scientific Company, Concord, California. Model 3100 Console Analog Computer Instruction Manual. June, 1960.

12. Etherington, H. (ed.). Nuclear Engineering Handbook. McGraw-Hill, 1958.

13. Gibson, J. E. Nonlinear Automatic Control. McGraw-Hill, 1963.

14. Glasstone, S. and M. C. Edlund. The Elements of Nuclear Reactor Theory. D. Van Nostrand Co., 1952.

5. Handler, H. E., Associate Professor of Physics, U. S. Naval Postgraduate School. Private Conversation and Class notes.

6. Harrer, J. M., Nuclear Reactor Control Engineering. D. Van Nostrand Co., 1963.

7. Harrer, J. M. and J. A. Deshong, Jr., Discontinuous Servo for Control of Power Reactors. Nucleonics, V. 12, January, 1954: 44-51.

8. Hughes, D. J., and others. Delayed Neutrons from Fission of U^{235}. Physical Review, V. 73, No. 2, 1948: 111.

9. Keepin, G. R. and T. F. Wimett. Reactor Kinetic Functions: A New Evaluation. Nucleonics, V. 16, October, 1958: 86-90.

10. Keepin, G. R., T. F. Wimett and R. K. Zeigler. Delayed Neutrons from Fissionable Isotopes of Uranium, Plutonium and Thorium. Physical Review, V. 107 No. 4, 1957: 1044.

11. Millman, J. and H. Taub. Pulse and Digital Circuits. McGraw-Hill, 1956.

12. Oak Ridge National Laboratory. Applied Nuclear Physics Division, Annual Report for Period Ending September 10, 1956. Determination of Reactor Parameters from Period Measurements by R. Gwin. 84-85.

13. Schultz, M. A., Control of Nuclear Reactors and Power Plants. McGraw-Hill, 1961.

14. Thaler, G. J. and R. G. Brown. Analysis and Design of Feedback Control Systems. McGraw-Hill, 1960.

15. Thaler, G. J. and M. P. Pastel. Analysis and Design of Nonlinear Feedback Control Systems. McGraw-Hill, 1962.

16. United States Atomic Energy Commission. Reactor Handbook: Physics (Selected Reference Material on Atomic Energy, V. 2) Chapter 1.6 Reactor Dynamics by G. Goertzel. McGraw-Hill, 1955.

17. Argonne National Laboratory. Installation and Interference Problems in Reactor Instrumentation Systems, by W. K. Brookshier. August, 1958. Report No. ANL-5901.